Microemulsion-based Organogels Containing Inorganic Nanoparticles

Supporting Information

Kieran Trickett[1], Harriet Brice[1], Olesya Myakonkaya[1], Julian Eastoe*[1], Sarah E. Rogers[2], Richard K. Heenan[2], Isabelle Grillo[3]

[1] School of Chemistry, University of Bristol, Cantock's Close, Bristol, BS8 1TS

[2] ISIS STFC, Rutherford Appleton Laboratory, Chilton, UK OX11 0QZ

[3] Institut Max Von Laue Paul Langevin, F-38042 Grenoble, France

Synthesis of deuterated AOT

Deuterated 2-ethyl hexanol was purchased from the Oxford Isotope Facility. Maleic anhydride (1.0 eq.), deuterated alcohol (2.05 eq.), and toluene-4-sulfonic acid (0.1 eq.) were refluxed in toluene. A Dean and Stark trap was used to remove water produced from the esterification reaction and thus drive the equilibrium towards products. The reaction was considered complete when no further water was evolved. Once complete, the reaction mixture was cooled to 70°C and washed with hot water (6 x 50 ml) to remove un-reacted maleic anhydride and toluene-4-sulfonic acid. The crude diester was obtained by rotary evaporation to yield a yellow/brown liquid. The crude diester was then purified by flash chromatography giving a colorless liquid. Flash chromatography was carried out over SiO_2 using 10% Et_2O/PE as the solvent.

The purified diester (1.0 eq.) was dissolved in ethanol (5g/50ml) and water added to saturation. Sodium sulfite (1.8 eq.) and sodium metabisulfite (2.2 eq.) were added and the reaction mixture was refluxed for approximately six hours. The formation of the sulfosuccinate product was monitored by thin layer chromatography (TLC) eluting with ethyl acetate. After cooling, the solvent was removed by rotary evaporation. The resulting white solid was then dissolved in distilled ethyl acetate, the reaction mixture was then decanted off leaving any un-reacted salts in the reaction vessel. The crude surfactant was again obtained by rotary evaporation and left to dry overnight at 40°C and under vacuum (~ 10 mmHg). Final extraction of inorganic materials was achieved by means of methanol centrifugation. The dried surfactant was dissolved in the minimum amount of dried, doubly distilled methanol. Residual inorganic reagents were precipitated out, and separated by centrifugation at 25°C and 6000 rpm. The supernatant was decanted and any residual solids were discarded. The solvent was removed by rotary evaporation and left to dry overnight at 40°C and under vacuum (~ 10 mmHg). This process was repeated until no further inorganic residues were removed.

Nanoparticle Synthesis

There are a number of synthetic methods by which stable and size controlled nanoparticles can be prepared.[1, 2] Particularly successful has been the use of microemulsions[3] as reaction and stabilizing media, typically producing small and quite monodisperse nanoparticles.[4] The microemulsion droplets in these systems provide an environment for controlled nucleation and growth. Particle growth is limited by the rate of inter-micellar exchange and the steric stabilization provided by the surfactant prevents aggregation. The final size and shape of the nanoparticles can be controlled by simply changing the nature of the surfactant or composition of the system.[3]

Preparation of water absent surfactant-stabilised gold nanoparticles

A method based on that reported by Wilcoxon[5] was employed. Two microemulsions were prepared each containing a mixture of the anionic surfactant AOT and the non ionic surfactant hexaethylene glycol monododecyl ether, $C_{12}E_6$ (Sigma), in octane. The concentration of AOT was 0.05 M. The molar ratio of AOT to $C_{12}E_6$ was 80/20. To one microemulsion auric potassium tetrachloride ($KAuCl_4$ Sigma) was added at a concentration of 0.0012 M and to the other microemulsion sodium borohydride ($NaBH_4$) (Sigma) was added at a concentration of 0.017 M. On drop-wise addition of the reductant containing microemulsion, under stirring, a deep red color developed.

Preparation of surfactant stabilised Fe_3O_4 magnetic nanoparticles

Method based on that reported by Shen.[6] Quantities based on a 5 g synthesis. $FeCl_2.4H_2O$ (4.3 g) (Sigma) and $FeCl_3.6H_2O$ (11.8 g) (Sigma) were dissolved in degassed water under the protection of nitrogen. The solution was heated to 80°C with stirring. The surfactant lauric acid (0.5 g) (Sigma) dissolved in acetone (25 mL) (Sigma) was added during the heating process. 28% (w/w) NH_4OH (25 mL) was added once the solution had reached 80°C followed by five portions of lauric acid (1 g) in acetone (25 mL) over a period of five minutes. The solution was stirred for 30 minutes at 80°C then cooled slowly to room temperature. The suspension was precipitated with acetone (200 mL) and isolated by magnetic decantation. The precipitates were then washed with more acetone (100 mL) and again isolated by magnetic decantation. This washing-decantation process was repeated five times to remove excess lauric acid. The particles were then dried in air on a Petri dish.

Preparation of AOT coated silica nanoparticles in heptanes

The method used to prepare AOT coated silica nanoparticles dispersed in heptane was based on the drying method previously reported by Tabor.[7] The silica nanoparticles were supplied as 30 wt % dispersions in water. The required amount of water was added to form 6 wt % dispersions. A surfactant solution (6 wt % AOT) dissolved in ethanol was then added and the solution was sonicated for 30 minutes. Small aliquots of the solution were dried in a vacuum oven at 40°C for 12 hours then re-dispersed in heptane. Gentle centrifugation (120 s at 3000 rpm) was used to sediment out any large aggregates, and the final dispersion was decanted off.

Nanoparticle Characterization

TEM

TEM analysis of the prepared nanoparticles was carried out on a JEOL JEM 1200 EX Mk2 TEM with a standard tungsten filament, operated at 120 KV up to magnifications of 1 million. The images were recorded digitally using a MegaViewII digital camera and Soft Imaging Systems GmbH analySIS 3.0 image analysis software. Samples were deposited directly on carbon coated copper grids by application of a droplet of the nanoparticle-containing solution and evaporation of the solvent at room temperature. The solvents were all non-polar so wetting of the grid occurred readily. The particles were all essentially spherical in shape and with narrow size distributions. Table 1 (main paper) summarizes the particle sizes determined from TEM analysis for the different nanoparticles synthesized and the method used to prepare them. The sizes are in good agreement with the literature values for particles synthesized using those methods.[1, 5-7]

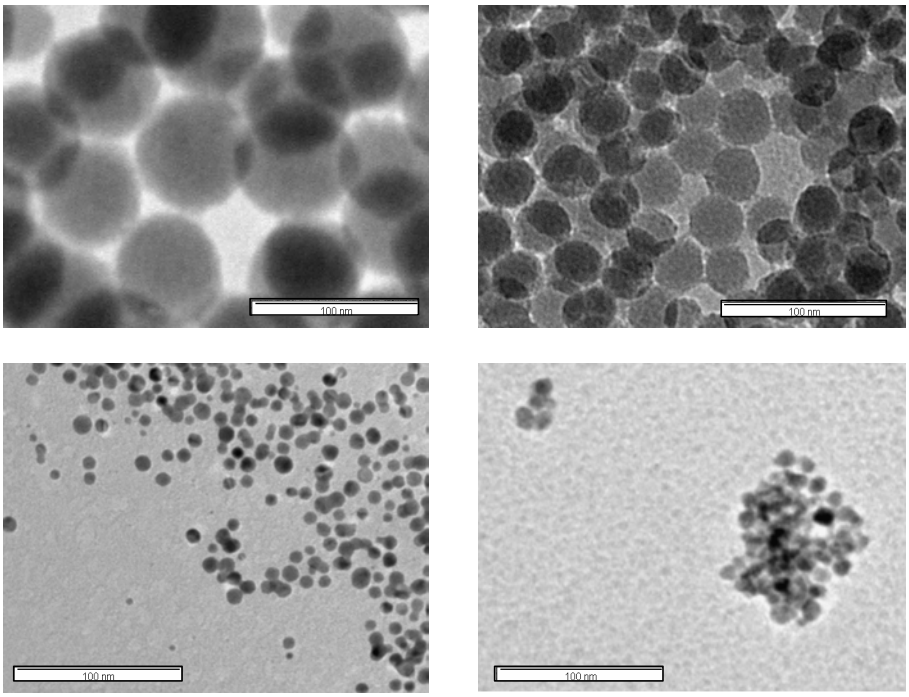

Figure S1: TEM images of (top left) 80 nm silica,(top right) 25 nm silica, (bottom left) gold nanoparticles, (bottom right) magnetite.

UV/Visible Spectroscopy

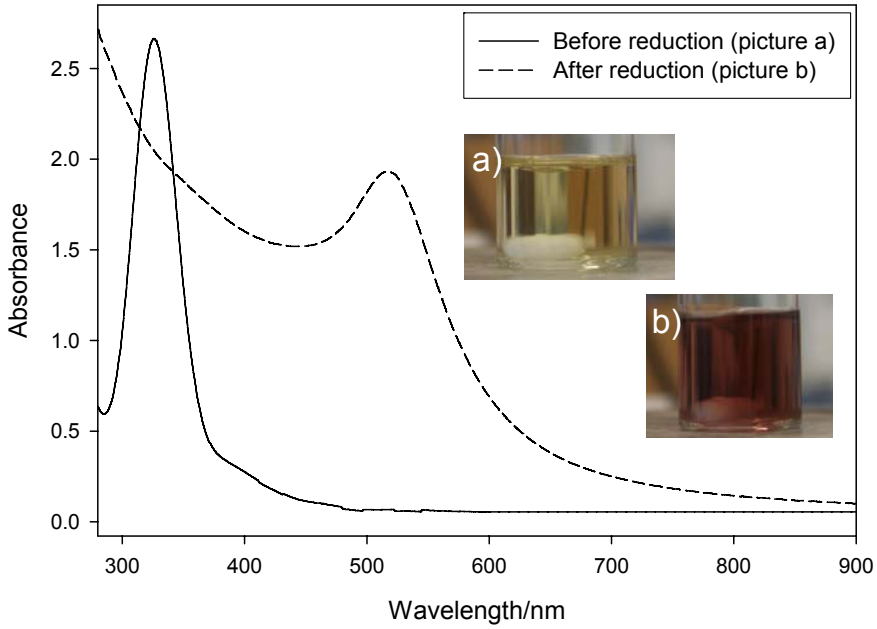

Figure S2: UV-visible absorbance spectra of microemulsions containing gold salt before and after reduction with sodium borohydride.

The optical properties of gold nanoparticles (Au-NPs) have been well characterized in the literature.[5] There is a strong dependence of the wavelength of maximum absorbance, λ_{max}, on the diameter of the particle diameter; for Au-NPs in the range 3-4 nm λ_{max} is less than 500 nm. For particle diameters of 5 nm to 40 nm λ_{max} is between 505 and 520 nm and for particle diameters larger than 40 nm λ_{max} > 530 nm.[5]

Figure S2 shows the UV-visible absorbance spectra of microemulsions containing the gold salt before and after the reduction process with sodium borohydride. The disappearance of the peak at 326 nm, which is associated with a d-d transition typical of the $AuCl_4^-$ ion[2], and appearance of the peak at 517 nm indicates reduction of the Au(III) ions and formation of gold nanoparticles. The λ_{max} for the gold nanoparticle solution at 517 nm is consistent with literature values for particle sizes between 5 and 40 nm.[5] This size range is in good agreement with gold nanoparticles previously synthesized by this method[5] and with TEM analysis, which indicate the particle sizes to be between 5 and 9 nm. Figure S3 shows UV-visible spectra of several gold nanoparticle solutions synthesized by the same method but at different times and one by a different operator showing good reproducibility. The gold nanoparticles are stable over time as shown in Figure S4.

Figure S5 shows the absorption spectra of various concentrations of Au-NPs which have been dried and re-dispersed in heptane. In all cases the λ_{max} does not change from that of the pre-dried gold solutions indicating that NPs can be dried and re-dispersed without detrimental effects on size and stability. The inset of Figure S5 shows a Beer-Lambert linear dependence of maximum absorbance with concentration, a relationship which is comparable to that observed in MBGs (see Figure 2 main paper).

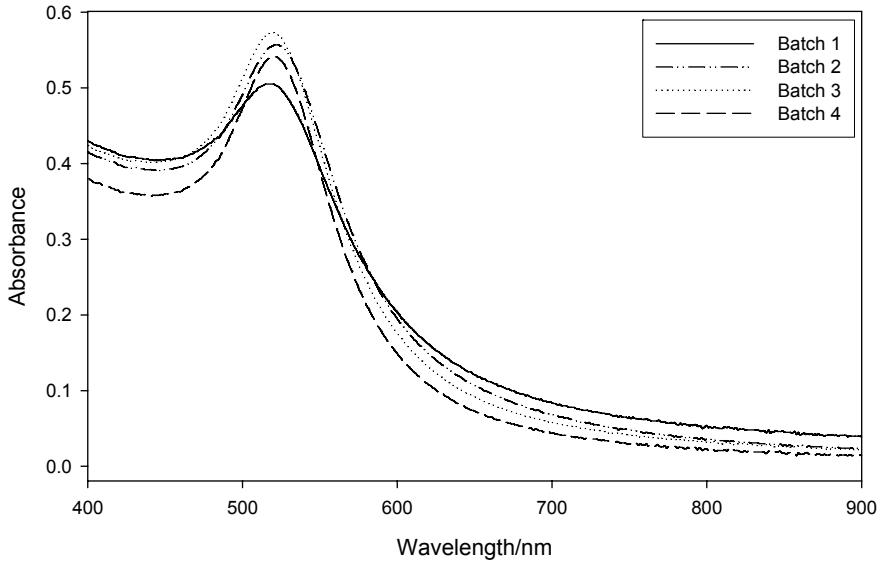

Figure S3: UV-visible absorbance spectra of several gold nanoparticle dispersions synthesized using the same method but at different times, and once by a different operator.

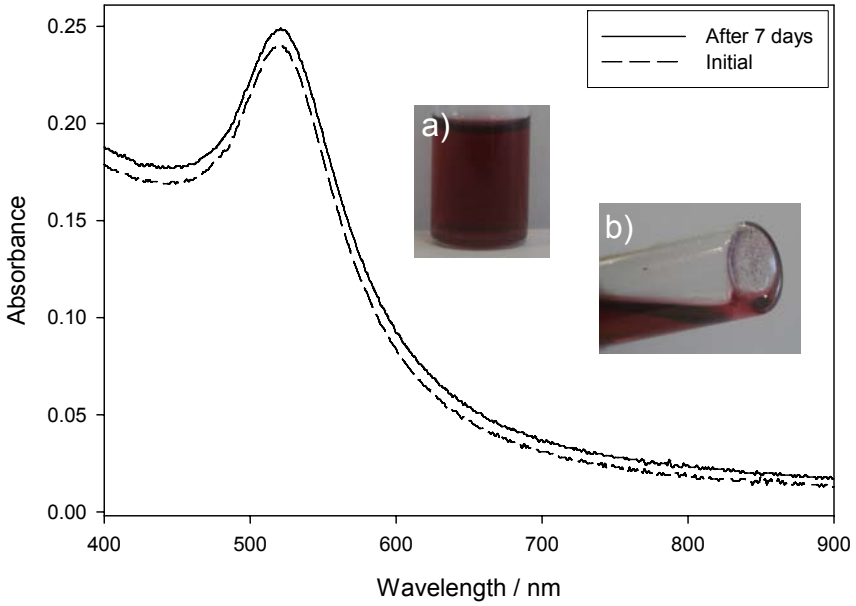

Figure S4: UV-visible absorbance spectra of gold nanoparticles in octane recorded initially and seven days after synthesis. Inset: photograph showing initial gold nanoparticle solution and a small amount of sedimentation that had occurred after 7 days.

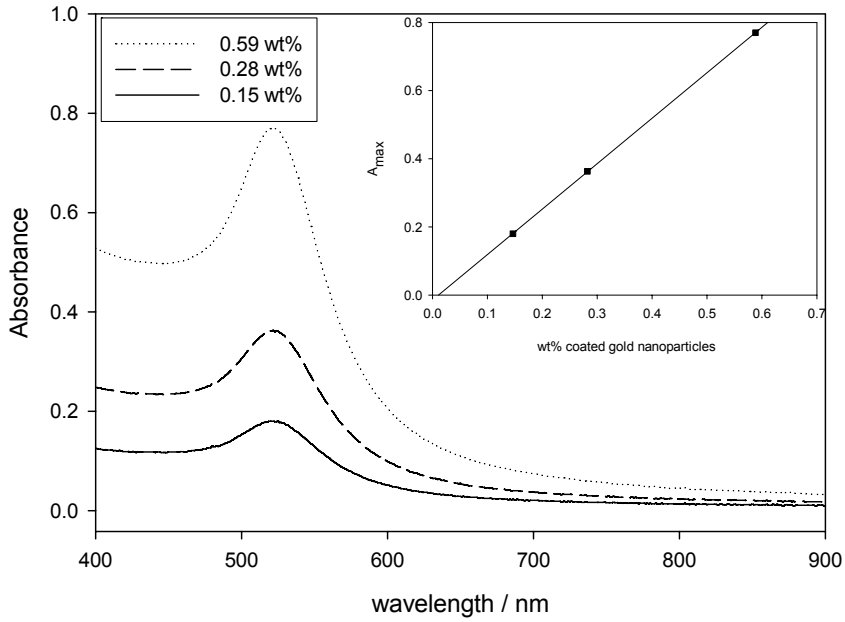

Figure S5: UV-visible absorption spectra of gold nanoparticles at different concentrations dispersed in heptane. Inset shows Beer-Lambert type dependence of absorbance with concentration.

Nanoparticles Dispersed in MBGs

UV/Visible Spectroscopy

The Au-NPs were quite stable in the MBG over a period of seven days as shown by the UV spectra (Figure S6).

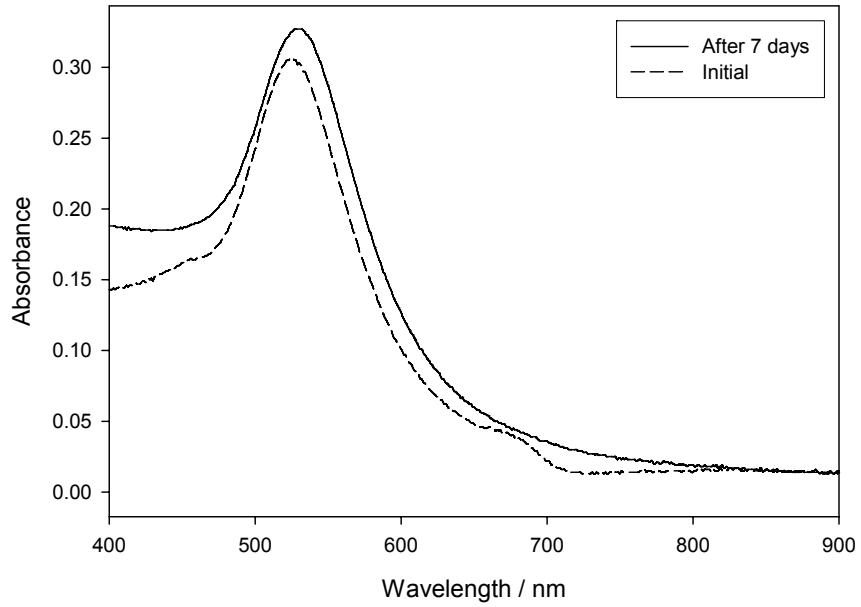

Figure S6: UV-visible absorbance spectra showing stability of Au-NPs dispersed in an MBG. Maximum absorbance wavelengths: initial sample λ_{max} = 524 nm, after 7 days sample λ_{max} = 529 nm. MBG composition: w = 60, 0.40 M AOT, 14% w/v gelatin.

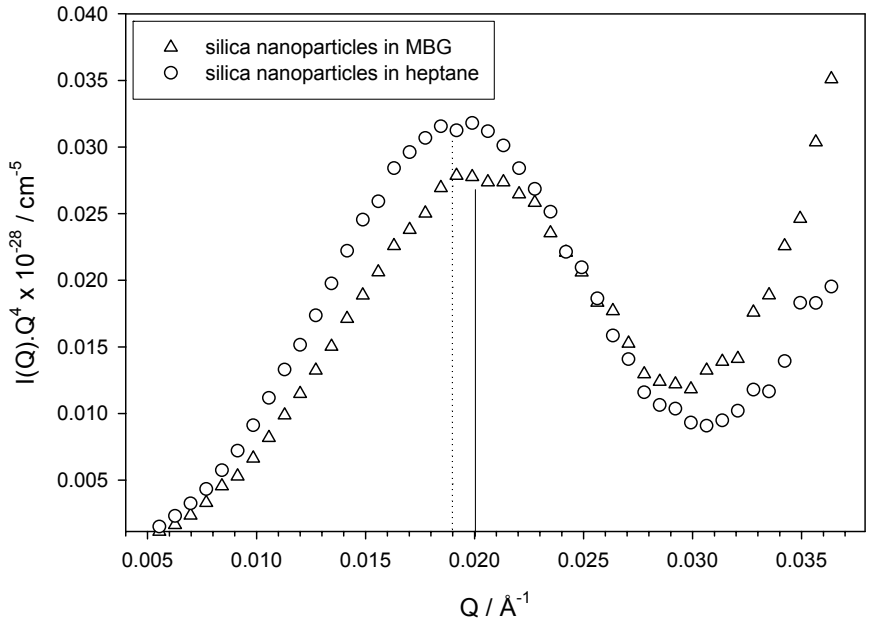

Figure S7: Porod analysis of SANS profiles described in main paper (Figure 1b) comparing the radius of silica nanoparticles dispersed in heptane and MBGs. Calculated radii can be found in Table S1. ~2.5wt% silica nanoparticles stabilized by deuterated AOT dispersed in pure h-heptane and a fully hydrogenated MBG . $Q_{porod}^{max} = \frac{2.7}{radius}$

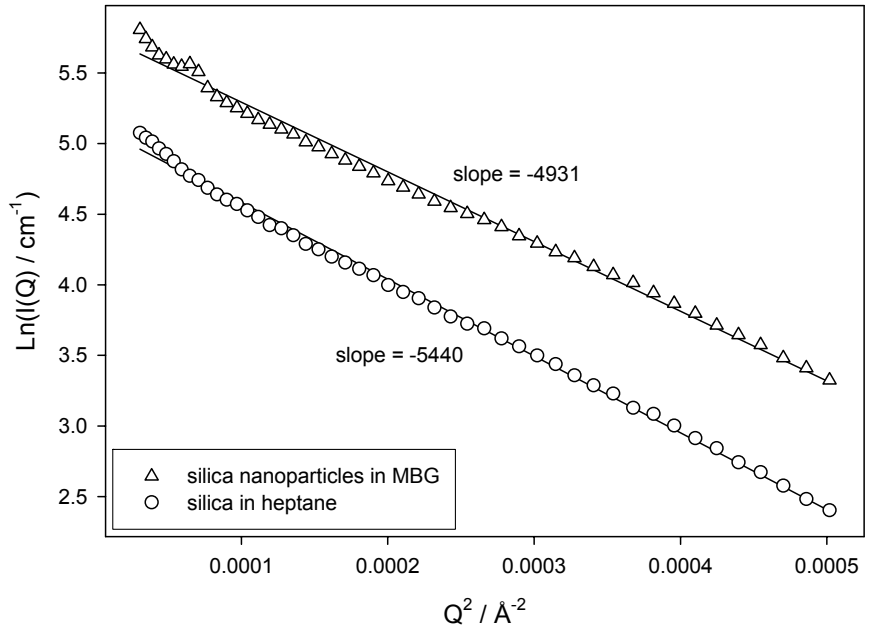

Figure S8: Guinier analysis of SANS profiles described in main paper (Figure 1b) comparing the radius of silica nanoparticles dispersed in heptane and MBGs. Calculated radii can be found in Table S1. ~2.5wt% silica nanoparticles stabilized by deuterated AOT dispersed in pure h-heptane and a fully hydrogenated h-MBG. $sphere\ radius = \sqrt{(5 \times slope)}$

Figures S7 – S8 show Porod and Guinier analysis of the SANS profile for SiO_2-NPs dispersed in both fully hydrogenated heptane and MBG. The calculated radii for the core SiO_2 is consistent with values from model fitting discussed in the main paper Figure 1b. A comparison of the calculated radii from different analyses can be found in Table S1. The results show that the SiO_2-NPs remain essentially unchanged, whether they are dispersed in pure heptane or the more structured MBG.

Continuous Phase	Radius / Å			
	TEM	SANS Model Fitting	SANS Porod	SANS Guinier
Heptane	125 - 150	143	142	165
MBG	125 - 150	158	135	155

Table S1: Comparison of radii of silica nanoparticles dispersed in heptane and MBGs determined by different analyses.

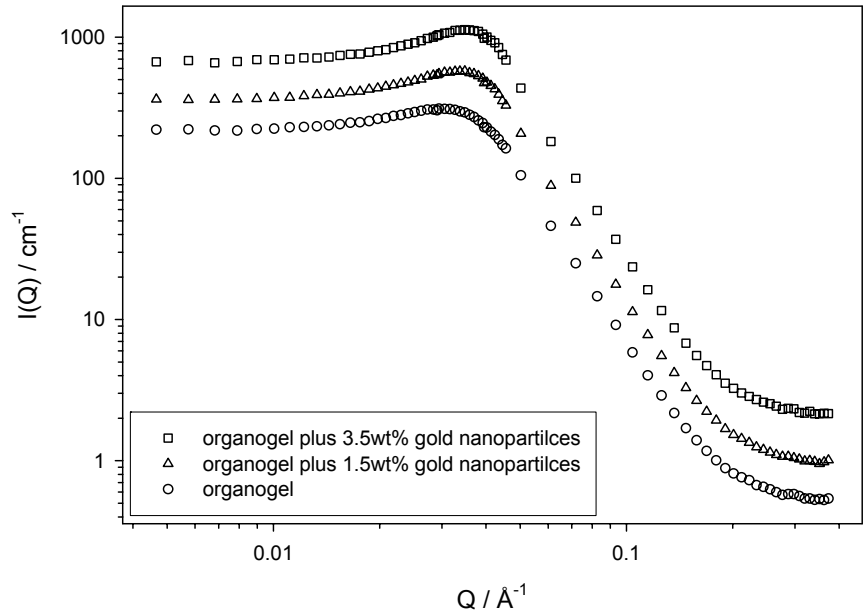

Figure S9: SANS profiles showing MBG with increasing amounts of gold nanoparticles. MBG composition: w = 60, 0.40 M AOT, 14% w/v gelatin.

SANS experiments were also performed on MBG samples of higher volume fractions containing increasing amounts of Au-NPs (Figure S9). The influence of the interparticle structure factor, *S(Q)*, at higher volume fractions acts to reduce the absolute scattering intensity in the low-Q region resulting in a peak in the SANS profile. The similarity in these SANS profiles shows, as with the SANS

results discussed in the main paper, that there is little change in the structure of the MBG on incorporation of Au-NPs. Given the influence of the interparticle structure factor it was not possible to obtain reliable structural parameters for the MBG for these profiles with higher Au-NP loadings.

SANS Models

The absolute scattering intensity, I(Q), for polydisperse, homogeneous solid-spheres can be written as[8]:

$$I(Q) = N_p[P(Q,R)p(R)]S(Q)$$

Where N_p is the particle number density, P(Q) is the single particle form factor, p(R) is a normalized distribution function (in this case a Schultz function), and S(Q) is the interparticle structure factor, which accounts for interactions.

Expressions for a form factor of a sphere of radius, r[8]:

$$P(Q,r) = 9V_p^2(\rho_{core} - \rho_{solvent})^2\left[\frac{\sin(Qr) - Qr\cos(Qr)}{Qr^3}\right]^2$$

and for a rod of radius, r, and length, L[9].

$$P(Q) = V_1p^12\ (\rho_1core - \rho_1solvent)^12\ \int_1 0^1(\pi/2)\ [([\sin^12\ (\pi(1/2)\ QL\ \cos\beta][4]J_1 1^12\ (QR\ \sin\beta)])/([\square(1/4$$

where V_p is the particle volume, $(\rho_{core} - \rho_{solvent})$ is the difference in neutron coherent scattering length density between the deuterated water droplet cores and the hydrogenated solvent. $J_1(x)$ is a Bessel function of the first kind and β is the angle between the scattering vector and the rod axis.

When dealing with the scattering from the silica spherical core-shell particles, the general form factor, P(Q, r), is given as[7, 10]:

$$P(Q,r) = \frac{16\pi^2}{9\left[(\rho_{shell} - \rho_{solvent})3r_d^3\left(\frac{\sin Qr_d - Qr_d\cos Qr_d}{(Qr_d)^3}\right) - 3r_c^3\left(\frac{\sin Qr_c - Qr_c\cos Qr_c}{(Qr_c)^3}\right)\right]^2} +$$

$$[(\rho_{\perp}core - \rho_{\perp}solvent)\ [3r]_{\perp c}{}^3\ ((\sin [Qr_{\perp}c] - Qr_{\perp}c\cos Qr_{\perp}c)/([(Qr]_{\perp c})^3))]^2$$

Where r_d is the particle (core + shell) radius, r_c the core radius, ρ_{shell}, $\rho_{solvent}$, ρ_{core} the scattering length density of the shell, solvent and core respectively. The shell thickness can be determined as $r_d - r_c$.

Application: Magnetic MBGs

Video footage of chunks of the magnetic MBGs with incorporated Fe_3O_4 particles. immersed in pure heptane and then being magnetically manipulated are available as files . Gel composition: 0.40 M AOT, 12% (w/v) gelatin w = 50.

References

(1) M. S. Lee, G.-D. Lee, C.-S. Ju and S.-S. Hong 2005, ***88***, 389.
(2) P. Calandra, C. Giordano, A. Longo and V. T. Liveri *Mater. Chem. Phys.,* 2006, ***98***, 494.
(3) J. Eastoe, M. J. Hollamby and L. Hudson *Adv. Colloid Interface Sci.,* 2006, ***128***, 5.
(4) Y. Mori, Y. Okastu and Y. Tsujimoto *J. Nanopart. Res.,* 2001, ***3***, 219.
(5) J. P. Wilcoxon, R. L. Williamson and R. Baughman *J. Chem. Phys.,* 1993, ***98***, 9933.
(6) L. F. Shen, P. E. Laibinis and T. A. Hatton *Langmuir,* 1999, ***15***, 447.
(7) R. F. Tabor, J. Eastoe, P. J. Dowding, I. Grillo, R. K. Heenan and M. Hollamby *Langmuir,* 2008, ***24***, 12793.
(8) M. Kotlarchyk and S. H. Chen 1983, ***79***, 2461.
(9) P. J. Atkinson, B. H. Robinson, A. M. Howe and R. K. Heenan *J. Chem. Soc. Faraday Trans.,* 1991, ***87***, 3389.
(10) M. Kotlarchyk, S.-H. Chen, J. S. Huang and M. W. Kim *Phys. Rev. A,* 1984, ***29***, 2054.